Chinese Chemical Letters 33 (2022) 2708–2710

Contents lists available at ScienceDirect

Chinese Chemical Letters

journal homepage: www.elsevier.com/locate/cclet

Applications of ambient electric arc ionization mass spectrometry in saline samples

Yuan Li[a,1], Yuanji Gao[a,b,1], Binpeng Zhan[a], Weiwei Chen[a], Fengjian Chu[a], Hongru Feng[a], Zhan Gao[a], Zihan Ma[a], Yuanjiang Pan[a,*]

[a] Department of Chemistry, Zhejiang University, Hangzhou 310027, China
[b] College of Chemistry and Materials Science, Sichuan Normal University, Chengdu 610068, China

ARTICLE INFO

Article history:
Received 19 June 2021
Revised 17 August 2021
Accepted 29 August 2021
Available online 4 September 2021

Keywords:
Electric arc
Ion source
Salinity tolerance
Mass spectrometry
Ambient electric arc ionization

ABSTRACT

Salinity tolerance of ambient electric arc ionization (AEAI) was evaluated by comparing electrospray ionization for various samples at NaCl concentrations from 0 to 1000 mmol/L. AEAI-mass spectrometry (AEAI-MS) exhibited an excellent signal intensity even at NaCl concentrations of 1000 mmol/L, while the ESI-MS had no signal because high salinity has a strong inhibitory effect on analytes. The sodium adduct was verified using LiCl instead of NaCl. AEAI-MS successfully quantified saline samples with an excellent quantitative ability ($R^2 \geq 0.998$). We also achieved some analytical samples in the buffer solution at a very high concentration and even in a saturated salt solution. Overall, AEAI-MS has protonated ions for most target analytes. In addition, the relationship between auxiliary temperature and the distance from the sample to the arc was investigated, and the results indicated that thermal desorption plays an important role in AEAI source.

There is a need to analyze saline sample in mass spectrometry (MS). Highly-saline samples cannot be directly analyzed by MS because of salt precipitation, which blocks cones and ion lenses. Moreover, the presence of salts severely suppresses MS signal and leads to salt cluster ions in the mass spectrum. However, salt unavoidably exists in many samples because of the production process and separation processes [1–4].

Over the years, various MS studies have tried to use different ion sources coupled to a mass spectrometer to directly analyze samples in complex matrices [5–20]. Compared to traditional electrospray ionization (ESI), desorption nanoelectrospray ionization (nanoDESI) exhibits better MS signal intensities for samples with salt contamination due to the decrease in the number of droplet fissions causing unnecessary salts enrichment [21]. Signal-to-noise ratios do not substantially deteriorate even at NaCl concentrations of 2.5 mol/L. Based on dielectric barrier discharge ionization (DBDI), a capillary electrophoresis (CE) MS interface exhibits a higher tolerance for non-volatile salts and surfactants [22]. In addition, a centimeter-scale continuous silica isoporous membrane is integrated into a facile microfluidic chip for protein desalting based on a dialysis principle before MS analysis. Notably, this device achieved approximately 99% desalting efficiency for the isotonic saline sample at a flow rate of 1 μL/min while protein loss was only 5% [23].

The arc plasma-based dissociation (APD) device is a newly developed ionization technique. An electric arc with a voltage ranged between 15–20 kV is used to induce the dissociation of neutral molecules or ions generation by arc discharges. Elimination and aromatization were observed as special dissociation patterns in this device, which can be applied in isomer differentiation [24]. It is worth noting that, based on previous researches on arc and plasma [25-29], an AEAI source [30] at a voltage of 7 kV with soft ionization characteristics was established. We further evaluated the detection ability of AEAI for samples with high salt or buffer solution concentrations. It is essential that AEAI ionize analytes in complex matrices such as biological samples.

Herein, saline samples were analyzed using AEAI-MS. Mesterolone is a dihydrotestosterone derived anabolic androgenic steroid and is generally used to treat male hypogonadism. Fig. 1 shows the ESI and AEAI mass spectra of 10 μg/mL mesterolone samples at different NaCl concentrations, respectively. Figs. S1-S4 (Supporting information) support universality of the phenomenon. For high-salt samples, the AEAI mass spectrum exhibited a stronger MS response compared to ESI. At NaCl concentrations of 1000 mmol/L, there was no mesterolone peak in the ESI mass spectrum, while a high protonated peak was observed in the AEAI

* Corresponding author.
E-mail address: panyuanjiang@zju.edu.cn (Y. Pan).
[1] These authors contributed equally to this work.

https://doi.org/10.1016/j.cclet.2021.08.119
1001-8417/

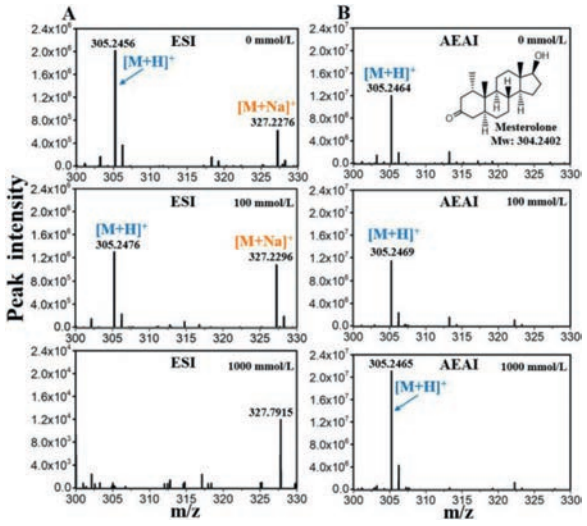

Fig. 1. (A) ESI and (B) AEAI mass spectra of mesterolone in 0, 100, and 1000 mmol/L NaCl solutions (10 μg/mL).

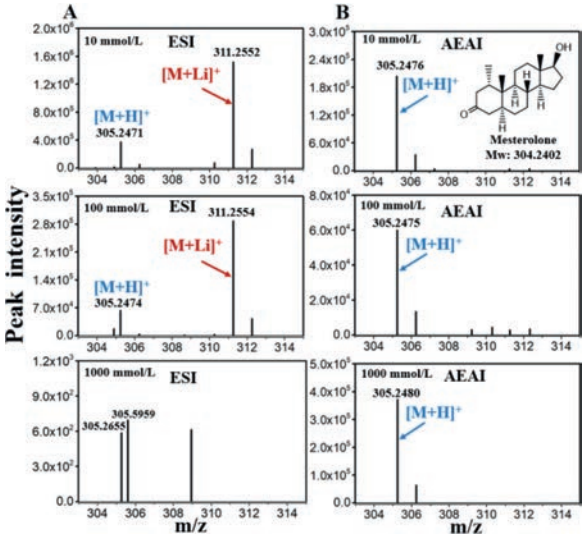

Fig. 2. (A) ESI and (B) AEAI mass spectra of mesterolone in 10, 100 and 1000 mmol/L LiCl solutions (10 μg/mL).

mass spectrum. In addition, for samples with 100 mmol/L NaCl or frequent uses of ESI, salt precipitation accumulates onto the surface of the MS inlet. Notably, this phenomenon did not occur during the AEAI process because AEAI has high ionization efficiencies with very small injection volumes (0.1–0.5 μL). Sodium adduct ions ($[M + Na]^+$) are obtained from samples containing NaCl in the ESI mass spectrum. As NaCl concentrations increase, the abundance of sodium adduct ion increases, while there is almost no sodium adduct ion in the AEAI mass spectrum.

Sodium adduct ions in the laboratory may interfere with analytical results, therefore, we used lithium ion to verify the sodium source. Fig. 2 shows that as LiCl concentration increases, the relative abundance of $[M + Li]^+$ in the ESI mass spectrum increases, thereby making it difficult to detect mesterolone at high-salt concentrations. The other sample results are provided in Figs. S5-S7 (Supporting information). AEAI has excellent salt tolerance and can hardly be affected by different types of metal ions in solution compared to ESI. Lithium chloride is weakly alkaline in aqueous solution, which is not conducive to providing protons for analytes [31].

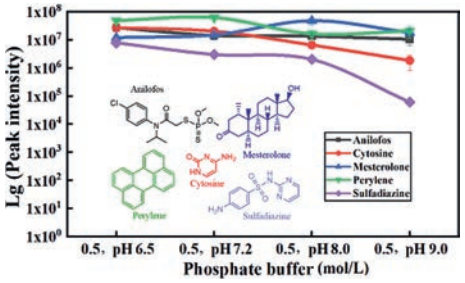

Fig. 3. MS signal intensities of anilofos, cytosine, mesterolone, perylene, and sulfadiazine in pH 6.5, pH 7.2, pH 8, and pH 9 phosphate buffers (0.5 mol/L) analyzed by the AEAI source. Error bars represent standard deviations for samples analyzed in triplicates.

Therefore, the intensity of the protonated peaks diminished with the use of AEAI.

Sulfadiazine is an antibiotic. Fig. S8 (Supporting information) shows quantitative curves of mesterolone and sulfadiazine from 0.10μg/mL to 10 μg/mL at 100 mmol/L NaCl solution, indicating that AEAI has good quantitative abilities in saline solution. According to the criteria specified by the European Commission Decision 2002/657/EC, limits of detection (LODs) were estimated based on the standard deviation (SD) obtained through the analysis of 20 spiked blank samples (LOD = 2.33 SD). The LOD for both mesterolone and sulfadiazine at 100 mmol/L NaCl solution was 3 ng/μL (0.1 μL).

We tested salinity tolerance for five standards with different polarities including anilofos, cytosine, mesterolone, perylene, and sulfadiazine under several extreme conditions, as shown in Figs. S9 and S10 (Supporting information). Perylene is a representative non-polar polycyclic aromatic hydrocarbon. We found that AEAI-MS can detect protonated ions of target analytes in high-concentration buffers or in saturated salt solutions. However, due to the degree of salt interference, the intensities vary with different salt concentrations.

Fig. 3 shows analytes in 0.5 mol/L phosphate buffers at pH values from 6.5 to 9.0. Results showed that MS signal intensities of anilofos, mesterolone, and perylene did not exhibit obvious changes with increasing pH values, while the MS signal intensity of cytosine and sulfadiazine decreased with increasing pH values. This is because cytosine and sulfadiazine molecules contain amino groups. Alkalinity of the solution inhibits the protonation process, therefore, there is no such phenomenon for the other three analytes without the amino groups.

Furthermore, as a type of thermal plasma with a high energy and rich charges, the arc ionization is attributed to a desorption ionization mechanism. In addition, a suitable desorption temperature improves the mass spectrometric signal, whereas high temperatures destroy analyte structures. Thermal burst ionization (TBI) [32] and fast shot desorption ionization (FEDI) [33] generated ions in the process of violent and high-speed eruption in a small space. Therefore, an auxiliary hot air gun was used to replace the heat of the remote arc to verify the importance of heating desorption for the AEAI source (Fig. 4A and Fig. S11 in Supporting information). We used the X axis movable platform to change the distance between the MS inlet and the arc (d2), and the distance from the arc to the sample (d1). The muzzle of hot air gun was placed about 10 mm away from the capillary to heat the sample to target temperature. It is noteworthy that the distance between the arc and MS inlet should be further than 2 mm to avoid discharge risking the mass spectrometer. Electrical safety in the atmospheric environment also needs be executed according to the specifications in laboratory.

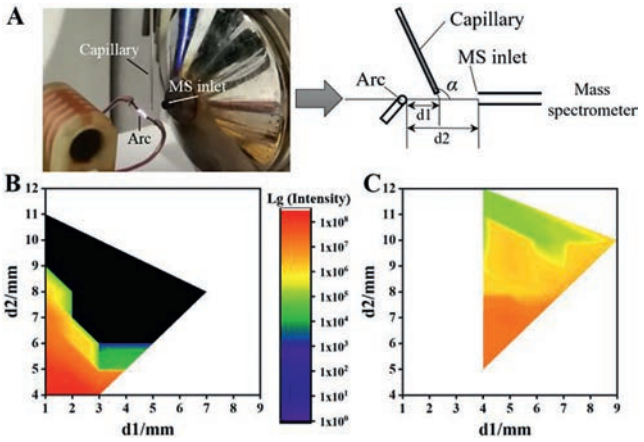

Fig. 4. (A) Photograph and schematic diagram of the established AEAI coupled with an LTQ Orbitrap mass spectrometer. Signal intensities of cytosine in different d1 (distance between arc and capillary) and d2 (distance between the arc and the MS inlet) positions as analyzed by AEAI-MS: (B) No heating; (C) At heating temperatures of 300 °C by hot air gun.

When we used the thermocouple to detect the temperature, we found that the actual temperature close to the set temperature could be obtained at 1-2 mm of the front end of the hot air gun. As shown in Fig. 4B, the signal was only found in a small range without heating source. As d2 increased, signal intensity decreased. This was attributed to subuliform ions diffusion. As d1 increased, the signal intensity also decreased. With the capillary heated to 300 °C using a hot air gun (Fig. 4C), signal intensities decreased with increasing of d1 and d2. Nonetheless, better signals were observed in a larger range, thereby verifying the significant effect of heat in AEAI. The temperature at 1 mm near the arc was about 440 °C, about 300 °C at 2 mm, and about 100 °C at 3 mm. The heating temperature from 100 °C to 450 °C at d1 of 7 mm and d2 of 8 mm away from the arc had no effect on the capillary. Signal intensities at different temperatures were similar and without obvious regularity, and were significantly greater than those without heating. In the end, 300 °C was selected as the optimal desorption temperature. When the arc was removed and the sample was heated to 300 °C only with the hot air gun, no ionization products can be observed under the same experiment. The d1 was greater than 3 mm (the hot air gun has a certain volume of 3 mm). The wind from the hot air gun caused the arc whisker to fluctuate, thereby affecting mass spectrometric results by negatively impacting the increase in d2 and being advantageous to the heating source. AEAI are ambient ion sources based on APCI mechanism. The electric arc provides adequate heat for the thermal desorption of analytes in high-salt sample. Electric arc ionization region can make the salt precipitation to fall off and avoid contaminating the instrument, and the vapor-phase analytes are then converted into cations via the reaction with the reactive charged species (mainly protonated water cluster ions) in the arc plasma. The analyte ions eventually migrate into the MS inlet and a clear mass spectrum is recorded.

In conclusion, we proved the performance and characteristics of AEAI to salinity tolerance and evaluated its mechanisms. In addition, AEAI exhibited better salinity tolerance (without obvious salt precipitation) than the traditional ESI source. Excellent AEAI-MS signals were obtained without salt cluster ions even at high-salt samples. Compared to the other desalination methods, such as two-dimensional liquid chromatography, and microfluidic chip desalination among others, AEAI exhibited direct analysis abilities for saline samples with minimum sample loss. This study informs the development of a convenient interface between liquid chromatography and MS for saline samples.

Declaration of competing interest

The authors declare that they have no known competing financial interests or personal relationships that could have appeared to influence the work reported in this paper.

Acknowledgments

This research was supported by the China State Key Research Program (No. 2016YFF0200503), National Natural Science Foundation of China (No. 21927810), and Sichuan Normal University (Nos. SYJS2020010 and KFSY2020004).

Supplementary materials

Supplementary material associated with this article can be found, in the online version, at doi:10.1016/j.cclet.2021.08.119.

References

[1] T.M. Annesley, Clin. Chem. 49 (2003) 1041–1044.
[2] J. Hu, Q.Y. Guan, J. Wang, et al., Anal. Chem. 89 (2017) 1838–1845.
[3] Z. Wang, H.J. Zhu, G.M. Huang, Rapid Commun. Mass Spectrom. 31 (2017) 1957–1962.
[4] R. Juraschek, T. Dülcks, M. Karas, J. Am. Soc. Mass Spectrom. 10 (1999) 300–308.
[5] D.Y. Chang, C.C. Lee, J. Shiea, Anal. Chem. 74 (2002) 2465.
[6] K.J. Fountain, M. Gilar, J.C. Gebler, Rapid Commun. Mass Spectrom. 18 (2004) 1295–1302.
[7] A.U. Jackson, N. Talaty, R.G. Cooks, G.J. Van Berkel, J. Am. Soc. Mass Spectrom. 18 (2007) 2218–2225.
[8] N. Na, M.X. Zhao, S.C. Zhang, C.D. Yang, X.R. Zhang, J. Am. Soc. Mass Spectrom. 18 (2007) 1859–1862.
[9] G.Y. Li, G.M. Huang, J. Mass Spectrom. 49 (2014) 639–645.
[10] B.W.J. Pirok, D.R. Stoll, P.J. Schoenmakers, Anal. Chem. 91 (2019) 240–263.
[11] Z. Takats, J.M. Wiseman, B. Gologan, R.G. Cooks, Science 306 (2004) 471–473.
[12] I.L. Arnaud, J. Josserand, H. Jensen, et al., Electrophoresis 26 (2005) 1650–1658.
[13] H.W. Chen, A. Venter, R.G. Cooks, Chem. Commun. 19 (2006) 2042–2044.
[14] K. Hiraoka, K. Nishidate, K. Mori, D. Asakawa, S. Suzuki, Rapid Commun. Mass Spectrom. 21 (2007) 3139–3144.
[15] A. Venter, M. Nefliu, R.G. Cooks, Trends Anal. Chem. 27 (2008) 284–290.
[16] M.K. Mandal, L.C. Chen, Y. Hashimoto, Z. Yuac, K. Hiraoka, Anal. Methods 2 (2010) 1905–1912.
[17] H. Wang, J.J. Liu, R.G. Cooks, Z. Ouyang, Angew. Chem. Int. Ed. 49 (2010) 877–880.
[18] Y. Akiyama, Y. Takahashi, I. Akutagawa, et al., Int. J. Mass Spectrom. 306 (2011) 37–43.
[19] Y.D. Zhang, X.J. Li, H.G. Nie, et al., Anal. Chem. 87 (2015) 6505–6509.
[20] S.T. Xu, Y.D. Zhang, L.N. Xu, Y. Bai, H.W. Liu, Analyst 141 (2016) 5913–5921.
[21] L. Hartmanová, P. Fryčák, M. Soural, et al., J. Mass Spectrom. 49 (2014) 750–754.
[22] Y.D. Zhang, W.P. Ai, Y. Bai, et al., Anal. Bioanal. Chem. 408 (2016) 8655–8661.
[23] W.H. Wu, D.X. Zhang, K.X. Chen, et al., Anal. Chem. 90 (2018) 14395–14401.
[24] S.Z. Zhu, L. Zhang, J. Zhang, Y.L. Guo, Anal. Chem. 92 (2020) 14633–14639.
[25] J. Heberlein, J. Mentel, E. Pfender, J. Phys. D: Appl. Phys. 43 (2010) 023001.
[26] J.H. Gross, Anal. Bioanal. Chem. 406 (2013) 63–80.
[27] X.J. Li, X. Wang, L.N. Li, Y. Bai, H.W. Liu, Mass Spectrom. Lett. 6 (2015) 1–6.
[28] X.P. Liu, H.Y. Wang, J.T. Zhang, et al., Sci. Rep. 5 (2015) 16893.
[29] H. Lu, Y.Y. Yin, J.H. Sun, et al., Chin. Chem. Lett. 32 (2021) 3457–3462.
[30] Y.J. Gao, Y. Li, B.P. Zhan, et al., Analyst 146 (2021) 5682–5690.
[31] R. Chen, L. Li, J. Am. Soc. Mass Spectrom. 12 (2001) 832–839.
[32] J.Y. Pei, K.F. Yu, Y.H. Wang, RSC Adv. 6 (2016) 2496–2499.
[33] X.P. Liu, H.Y. Wang, G.Q. Dong, et al., J. Am. Soc. Mass Spectrom. 29 (2018) 1319–1322.